

# Partition theory: A very simple illustration

Morrel H. Cohen

*Department of Physics and Astronomy, Rutgers University,  
126 Frelinghuysen Rd., Piscataway, NJ 08854, USA and*

*Department of Chemistry, Princeton University, Washington Rd., Princeton, NJ 08544, USA*

Adam Wasserman

*Department of Chemistry and Chemical Biology,  
Harvard University, 12 Oxford St., Cambridge MA 02138, USA*

Kieron Burke

*Department of Chemistry, University of California at Irvine,  
1102 Natural Sciences 2, Irvine, CA 92697, USA*

We illustrate the main features of a recently proposed method based on ensemble density functional theory to divide rigorously a complex molecular system into its parts [M.H. Cohen and A. Wasserman, *J. Phys. Chem. A* **111**, 2229 (2007)]. The illustrative system is an analog of the hydrogen molecule for which analytic expressions for the densities of the parts (hydrogen “atoms”) are found along with the “reactivity potential” that enters the theory. While previous formulations of Chemical Reactivity Theory lead to zero, or undefined, values for the chemical hardness of the isolated parts, we demonstrate they can acquire a finite and positive hardness within the present formulation.

## 1. INTRODUCTION

In a series of recent papers [1–3], two of us have developed a rigorous method for dividing a complex system into its parts based on density-functional theory [4–8]. The underlying theory, partition-theory (PT), was used to construct a formulation of chemical reactivity theory (CRT) [3] which, for the first time, is consistent with the underlying density-functional theory [8, 9] and is richer in structure than the preexisting CRT [10–13].

In PT [1–3], a sharp definition of the individual parts into which the whole system is partitioned is achieved first by selecting the nuclei of each putative part and maintaining these in the positions in which they occur in the whole and then requiring that the sum of the electron densities of the parts, each of which is treated as though isolated, add up exactly to the electron density of the whole (the density constraint). The electron densities of the parts are then to be determined by minimizing the sum of the density functionals of the individual parts with respect to the densities of the parts subject to the density constraint. The density functional used, that of ref.[8] (PPLB), allows for the existence of noninteger numbers of electrons on each part, necessary e.g. for the definitions of electronegativity [12] and hardness [13], key indices of chemical reactivity [3], and for incorporating covalent bonding between inequivalent parts.

The minimization proceeds via a Legendre transformation, which introduces a reactivity potential  $v_R(\mathbf{r})$  as the Lagrange multiplier of the density constraint. Thus, the formalism can become computationally complex. First the electron density of the whole system must be determined. Then, the densities of the parts must be determined simultaneously with  $v_R$ , all of which is required to set the stage for the determination of mutual reactivi-

ties between parts, though certain self-reactivities can be determined for each species alone without reference to a larger system [3].

Accordingly, in the present paper, we develop the partition theory in detail for an extremely simple system to exhibit its main features explicitly. The illustrative system is an analog of the hydrogen molecule in which the electrons move in one dimension along the molecular axis without interacting, and the nuclear Coulomb potentials are replaced by attractive delta-function potentials. As a consequence of these extreme simplifications, many quantities of interest can be determined analytically in a transparent manner, including the electron density of the molecule, of its parts (the “atoms”), and the reactivity potential at all internuclear separations.

In Section 2, the model is defined and the molecular density obtained. In Section 3, the parts are defined, shown to have one electron each, and a polar representation for their wave functions found which facilitates the minimization. In Section 4, the minimization is carried out, resulting in an Euler equation for the polar angle  $\beta(x)$  of that representation.  $\beta(x)$  is found in Section 5 and used to determine the reactivity potential  $v_R$  in Section 6. The principle of electronegativity equalization formulated in refs.[2] and [3] is shown to hold in Section 7. Also in Section 7, the hardness [3] of the isolated H atom is calculated, shown to be nonzero, and correlated with the strength with which its electron is bound. Thus, despite the fact that the model is a caricature of the real system, meaningful features of the partition theory are indeed illustrated by it, as discussed in the concluding Section, 8.

## 2. 1D-H<sub>2</sub>; INDEPENDENT ELECTRONS MOVING IN ATTRACTIVE $\delta$ -FUNCTION POTENTIALS IN ONE DIMENSION

Our task is to partition an analog of the H<sub>2</sub> molecule in which two electrons move independently in  $\delta$ -function nuclear potentials in one dimension into parts, analogs of H atoms. Each H atom has, by symmetry, only one electron, so the need for the PPLB density functional is avoided. Indeed no explicit use of density-functional theory is required for either the molecule or the atoms. The ground-state wave function  $\psi_0$  and energy  $E_0$  of an isolated H atom are (atomic units are used throughout):

$$\psi_0(x) = \sqrt{Z} e^{-Z|x|} , \quad (2.1)$$

$$E_0 = -Z^2/2 . \quad (2.2)$$

In Eq.(2.1),  $(-Z)$  is the strength of the  $\delta$ -function potential. To draw the analogy closer to real hydrogenic atoms, one could equate  $Z$  to the nuclear charge.

The ground-state energy  $E(N = 1)$  of one electron moving independently in the two  $\delta$ -function potentials centered at  $x = \pm a$  is  $E(N = 1) = -\kappa^2/2$ , where  $\kappa$  satisfies

$$\kappa = 2Z/(1 + \tanh \kappa a) . \quad (2.3)$$

The corresponding wavefunction is:

$$\psi_M(x) = \left. \begin{aligned} & B e^{\kappa(a-|x|)} , \quad |x| > a \\ & B \frac{\cosh \kappa x}{\cosh \kappa a} , \quad |x| < a \end{aligned} \right\} , \quad (2.4)$$

where

$$B = \kappa^{1/2} \left[ 1 + \frac{\kappa a}{\cosh^2 \kappa a} + \tanh \kappa a \right]^{-1/2} ; \quad (2.5)$$

Note that  $\kappa \rightarrow 2Z$  as  $a \rightarrow 0$  (united atom limit) and  $\kappa \rightarrow Z$  as  $a \rightarrow \infty$  (separated atom limit).

The two-electron molecular electron density is given by:

$$n_M(x) = 2 |\psi_M(x)|^2 , \quad (2.6)$$

and the total energy of the molecule is

$$E_M(N = 2) = 2E_M(N = 1) = -\kappa^2 , \quad (2.7)$$

where  $N$  is the number of electrons in the molecule. The chemical potential of the molecule is therefore

$$\mu_M = E(2) - E(1) = E(1) = -\kappa^2/2 . \quad (2.8)$$

## 3. PARITY DECOMPOSITION

We now partition the molecule into two parts  $\alpha = 1, 2$ , each having a real one-electron wave function  $\psi_\alpha$ , localized around  $-a$  and  $+a$  respectively, so that  $n_M(x)$  is given by

$$n_M(x) = n_1(x) + n_2(x) , \quad (3.1)$$

where  $n_\alpha(x)$  is the electron density of each part  $\alpha = 1, 2$  treated independently. The “atomic” wavefunctions are given by:

$$\psi_\alpha(x) = \sqrt{n_\alpha(x)} . \quad (3.2)$$

They are mirror images of each other,

$$\psi_2(x) = \psi_1(-x) , \quad (3.3)$$

and both are normalized.

We now decompose the  $\psi_\alpha$  into their symmetric,  $\psi_s(-x) = \psi_s(x)$ , and antisymmetric,  $\psi_a(-x) = -\psi_a(x)$ , parts by a rotation within the function space they span,

$$\psi_1 = \frac{1}{\sqrt{2}} (\psi_s + \psi_a) , \quad \psi_2 = \frac{1}{\sqrt{2}} (\psi_s - \psi_a) ; \quad (3.4)$$

$$\psi_s = \frac{1}{\sqrt{2}} (\psi_1 + \psi_2) , \quad \psi_a = \frac{1}{\sqrt{2}} (\psi_1 - \psi_2) . \quad (3.5)$$

The rotation leaves “lengths” within the space invariant so that

$$n_M = \psi_s^2 + \psi_a^2 . \quad (3.6)$$

We next introduce  $\beta = \beta(x)$ , a polar angle in the function space,

$$\psi_s = \sqrt{n_M} \cos \beta , \quad \psi_a = \sqrt{n_M} \sin \beta , \quad (3.7)$$

so that

$$\psi_{1,2} = \sqrt{n_M/2} (\cos \beta \pm \sin \beta) \quad (3.8)$$

Because the  $\psi_\alpha$  are non-negative,  $|\beta|$  cannot exceed  $\pi/4$ . Furthermore  $\beta$  must be an odd function of  $x$ , to ensure  $\psi_\alpha$  is also odd. This also guarantees normalization of  $\psi_\alpha$ .

## 4. THE EULER EQUATION FOR $\beta(x)$

To apply PT [2, 3], begin with the original Hamiltonian

$$H = \frac{1}{2} \sum_{i=1,2} p_i^2 - Z \sum_{i=1,2} [\delta(x_i - a) + \delta(x_i + a)] . \quad (4.1)$$

Then divide the system into overlapping regions, each with a given number of electrons. In this case, we choose one electron on the left, and the other on the right. Thus we have two 1-electron problems:

$$H_\alpha = \frac{p^2}{2} + v_\alpha , \quad v_{1,2} = -Z\delta(x \mp a) . \quad (4.2)$$

The PT problem is to minimize

$$\mathcal{E} = (\psi_1, H_1 \psi_1) + (\psi_2, H_2 \psi_2) , \quad (4.3)$$

subject to normalization of the wavefunctions, but also to the constraint that the total density equal the original molecular density, Eq.(3.1). (Without the latter constraint, we’d obviously find  $\psi_{1,2} = \psi_0(x = \mp a)$ ). In the

polar representation of Sec.3, both density and normalization constraints are automatically satisfied, so the partition problem becomes simply minimizing  $\mathcal{E}$  as a functional of  $\beta$ . That functional is

$$\mathcal{E} = \int dx \left\{ \frac{1}{2} \left[ \frac{1}{4} \frac{n_M'^2}{n_M} - \frac{1}{2} n_M'' + n_M (\beta')^2 \right] + \frac{1}{2} n_M [(v_1 + v_2) + (v_1 - v_2) \sin 2\beta] \right\}. \quad (4.4)$$

Varying it yields

$$\delta\mathcal{E} = \int dx \{ n_M \beta' \delta\beta' + (v_1 - v_2) n_M \cos 2\beta \delta\beta \}. \quad (4.5)$$

Integrating by parts, as usual, leads to

$$\delta\mathcal{E} = 2n\beta'\delta\beta|_{x=-\infty}^{x=+\infty} + \int dx \left\{ \frac{d}{dx} \left( n_M \frac{d\beta}{dx} \right) + (v_1 - v_2) n_M \cos 2\beta \right\} \delta\beta. \quad (4.6)$$

For  $\mathcal{E}$  to be stationary with respect to arbitrary variations  $\delta\beta$  of  $\beta$ , both terms contributing to  $\delta\mathcal{E}$  in Eq.(4.6) must vanish. The Euler equation which results from the vanishing of the second term in Eq.(4.6) is

$$-\frac{d}{dx} \left( n_M \frac{d\beta}{dx} \right) + (v_1 - v_2) n_M \cos 2\beta = 0, \quad (4.7)$$

$$\frac{d}{dx} \left( n_M \frac{d\beta}{dx} \right) + Z (\delta(x - a) - \delta(x + a)) \times n_M \cos 2\beta = 0. \quad (4.8)$$

The vanishing of the first term in Eq.(4.6) sets the boundary condition at infinity on the Euler equation (4.8). There are two possibilities, the vanishing of  $\beta'$  at infinity or the fixing of  $\beta$  there so that  $\delta\beta$  must vanish. As we shall see in Section 5, imposing the latter results in an unacceptable divergence in  $\beta'$  at infinity. We therefore impose the boundary condition

$$\beta'(x) = 0, \quad |x| = \infty. \quad (4.9)$$

## 5. SOLVING FOR $\beta(x)$

Eq.(4.8) becomes

$$\frac{d}{dx} \left( n_M \frac{d\beta}{dx} \right) = 0, \quad |x| \neq a, \quad (5.1)$$

subject to the boundary conditions Eq.(4.9) and

$$\left. \begin{aligned} \beta(a^-) &= \beta(a^+) \equiv \beta_a \\ \beta'(a^-) - \beta'(a^+) &= Z \cos 2\beta_a \end{aligned} \right\} x = a, \quad (5.2)$$

$$\left. \begin{aligned} \beta(-a^+) &= \beta(-a^-) = -\beta_a \\ \beta'(-a^-) - \beta'(-a^+) &= Z \cos 2\beta_a \end{aligned} \right\} x = -a. \quad (5.3)$$

The general solution of (5.1) is

$$\frac{d\beta(x)}{dx} = \frac{c_1}{n_M(x)}, \quad (5.4)$$

$$\beta(x) = \int^x dx' \frac{c_1}{n_M(x')} + c_2. \quad (5.5)$$

where  $c_1$  and  $c_2$  are constants. As implied above in Section 4, if  $c_1$  does not vanish  $\beta'$  diverges exponentially at infinity, according to Eq.(5.4), because  $n_M$  goes exponentially to zero, so, in accordance with Eq.(4.9),  $c_1$  vanishes for  $|x| > a$ , and  $\beta(x)$  is constant there,

$$\left. \begin{aligned} \beta(x) &= \beta_a, & x > a \\ &= -\beta_a, & x < -a \end{aligned} \right\}. \quad (5.6)$$

For  $|x| < a$  we can rewrite Eq.(5.6) as

$$\beta(x) = \int_{-a}^x dx' \frac{c_1}{n_M(x')} - \beta_a, \quad (5.7)$$

which implies that

$$\beta_a = \frac{1}{2} \int_{-a}^a dx \frac{c_1}{n_M(x)}. \quad (5.8)$$

From (5.8) we can relate  $c_1$  to  $\beta_a$  via Eq.(2.6),

$$c_1 = \frac{2\kappa B^2 \beta_a}{\cosh^2 \kappa a \tanh \kappa a}. \quad (5.9)$$

Inserting (5.9) for  $c_1$  into Eq.(5.4) and the result into the BC (5.2) or (5.3) produces an equation for  $\beta_a$ ,

$$\beta_a = \frac{Z}{2\kappa} \sinh 2\kappa a \cos 2\beta_a. \quad (5.10)$$

Inserting Eqs.(5.9) and (2.6) into Eq.(5.7) yields the remarkably simple result

$$\beta(x) = \frac{\tanh \kappa x}{\tanh \kappa a} \beta_a, \quad 0 < |x| < a. \quad (5.11)$$

Eqs.(5.6), (5.10), and (5.11), together with Eq.(2.3) provide a complete analytic solution for  $\beta(x)$  and through Eqs.(3.5) and (3.8) for the  $\psi_\alpha$ . In Fig.1 we show  $n_M$ ,  $n_1$  and  $n_2$  vs.  $x$  for  $Z = 1$  and  $a = 1$ . We see that each localized density spreads into the neighboring region, and looks quite similar to an atomic density. To see the differences from isolated atomic orbitals, in Fig.2 we make the distance smaller ( $a = 0.3$ ), and show the right-side ‘‘atomic’’ orbital  $\psi_1(x)$  (solid line) and compare it with the pure exponential orbital  $\psi_0(x)$  of Eq.2.1 (dashed line). The orbital  $\psi_1$  resembles  $\psi_0$  and tends to it for large  $a$ , but is distorted with respect to it for small  $a$ . Its maximum is still a cusp at  $x = a$ , but it also shows a second cusp at  $x = -a$ . Since  $\kappa > Z$  always (Eq.(2.3)), and either  $\psi_1$  or  $\psi_2$  is proportional to  $\psi_M$  for  $|x| > a$ , where  $\beta = \beta_a$  is constant, the PT atomic densities and orbitals decay more rapidly than isolated atoms. Since

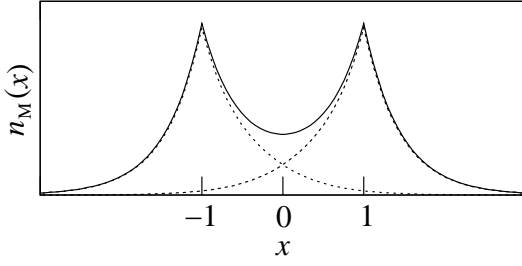


FIG. 1: Molecular density  $n_M(x)$  (solid), and “atomic” densities  $n_1(x)$  and  $n_2(x)$  (dotted) for  $Z = 1$  and  $a = 1$ .

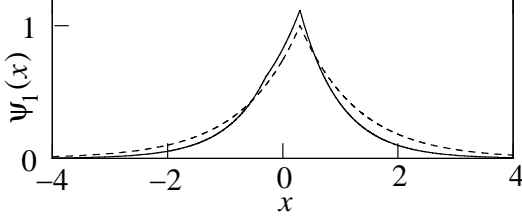


FIG. 2: Right-side “atomic” orbital  $\psi_1(x)$  (solid) and pure exponential orbital  $\psi_0(x)$  (dashed) for  $Z = 1$  and  $a = 0.3$ .

their normalization is the same, this in turn means enhanced density between the ‘nuclei’, due to bonding. In Fig.3, we show  $\beta(x)$  for  $Z = 1$ , and  $a = 0.1, 1$ , and  $10$ . Qualitatively, from Eq.(5.11),

$$\begin{aligned} \beta(x) &\simeq \beta_a \frac{x}{a}, \quad x < \min(1/\kappa, a) \\ &= \beta_a, \quad x > \min(1/\kappa, a) \end{aligned}$$

and if  $Za \gg 1$  (large separation),  $\beta_a \simeq \pi/4$  while if  $Za \ll 1$  (small separation),  $\beta_a \simeq a$ . The interpretation of these results is given in terms of (3.8), outside the bond region. If  $\beta_a$  is small, both ‘atoms’ share the density in each outside region. But if  $\beta_a$  is close to  $\pi/4$ , each atom dominates on its own side, consuming the entire density there.

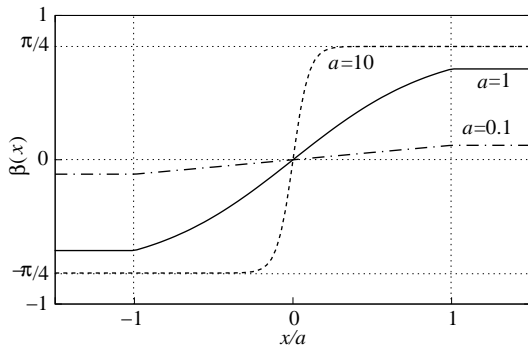


FIG. 3:  $\beta(x)$  vs.  $x$ , as given by Eq.(5.11), for fixed  $Z = 1$  and 3 different values of  $a$ .

## 6. THE REACTIVITY POTENTIAL

The one-electron wave functions  $\psi_1(x)$  and  $\psi_2(x)$  are not eigenstates of the part-Hamiltonians  $H_1$  and  $H_2$  of Eq.(4.2). The natural question arises: What are they eigenstates of? The partition theory of refs. [1–3] dictates that they are eigenstates of the modified single-electron Hamiltonians  $H_\alpha^R = p^2/2 + \mathcal{V}_\alpha$ ,  $\alpha = 1, 2$ :

$$\left(\frac{p^2}{2} + \mathcal{V}_\alpha\right) \psi_\alpha = \mu_M \psi_\alpha, \quad \alpha = 1, 2. \quad (6.1)$$

$$\mathcal{V}_\alpha = v_\alpha + v_R \quad (6.2)$$

where the eigenvalue, regardless of the part  $\alpha$ , is precisely equal to the molecular chemical potential  $\mu_M$  of Eq.(2.8). The potential  $v_R(x)$  is the *reactivity potential* that we now construct explicitly. Summing over  $\alpha$  and dividing by  $\psi_1 + \psi_2$  yields a symmetric expression for  $v_R$ ,

$$v_R = \mu_M - \frac{1}{\psi_1 + \psi_2} \frac{p^2}{2} (\psi_1 + \psi_2) - \frac{v_1 \psi_1 + v_2 \psi_2}{\psi_1 + \psi_2}. \quad (6.3)$$

$\psi_1$  and  $\psi_2$  can be reexpressed in terms of  $\psi_s$  and  $\psi_a$ , Eq.(3.5). Noting that

$$n_M = 2\psi_M^2, \quad (6.4)$$

using Eq.(3.7) for  $\psi_{s,a}$ , and taking the  $\delta$ -function character of  $v_\alpha$  into account results in

$$\begin{aligned} v_R &= \mu_M + \frac{1}{2\psi_M \cos \beta} \frac{d^2}{dx^2} (\psi_M \cos \beta) \\ &\quad - \frac{1}{2}(v_1 + v_2)(1 + \tan \beta_a). \end{aligned} \quad (6.5)$$

The molecular wave function  $\psi_M$  satisfies the Schrödinger equation,

$$-\frac{1}{2} \frac{d^2 \psi_M}{dx^2} + (v_1 + v_2) \psi_M = \mu_M \psi_M, \quad (6.6)$$

which can be used to transform Eq.(6.5) to

$$\begin{aligned} v_R &= -\frac{1}{2} \left\{ \left[ \frac{2}{\psi_M} \frac{d\psi_M}{dx} \frac{d\beta}{dx} + \frac{d^2 \beta}{dx^2} \right] \tan \beta + \left( \frac{d\beta}{dx} \right)^2 \right\} \\ &\quad + \frac{1}{2}(v_1 + v_2)(1 - \tan \beta_a). \end{aligned} \quad (6.7)$$

Using Eq.(6.4), the Schrödinger-like equation for  $\beta$ , Eq.(4.8), can be rewritten as

$$\begin{aligned} &-\frac{1}{2} \left[ \frac{2}{\psi_M} \frac{d\psi_M}{dx} \frac{d\beta}{dx} + \frac{d^2 \beta}{dx^2} \right] \\ &\quad + \frac{1}{2}(v_1 - v_2) \cos 2\beta_a = 0. \end{aligned} \quad (6.8)$$

Multiplying Eq.(6.8) by  $\tan \beta$ , invoking the oddness of  $\beta$  and the  $\delta$ -functions in  $v_1$  and  $v_2$ , and subtracting the result from Eq.(6.7) yields for  $v_R$

$$v_R = -\frac{1}{2} \left( \frac{d\beta}{dx} \right)^2 + \frac{1}{2}(v_1 + v_2) [1 - (1 + \cos 2\beta_a) \tan \beta_a]. \quad (6.9)$$

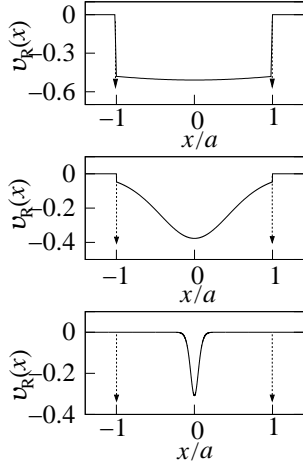


FIG. 4: Reactivity potential  $v_R$ , Eq.(6.10) for fixed  $Z = 1$  and 3 different values of  $a$ :  $a = 0.1$  (upper panel),  $a = 1$  (middle) and  $a = 10$  (bottom). The  $\delta$ -functions at  $\pm a$  are indicated by arrows.

Inserting our previous result for  $\beta(x)$ , Eqs.(5.6) and (5.11) into (6.9) yields an explicit result for  $v_R$ ,

$$v_R = \frac{\mu_M \beta_a^2}{\tanh^2 \kappa a} \frac{\theta(a - |x|)}{\cosh^4 \kappa x} + \frac{1}{2}(v_1 + v_2)[1 - \sin 2\beta_a] \quad , \quad (6.10)$$

where  $\theta(y) = 0$  for  $y < 0$ , 1 for  $y > 0$  is the Heaviside step function. Eq.(6.10) shows that  $v_R(x)$  vanishes for  $|x| > a$ , has attractive  $\delta$ -functions at  $\pm a$  whose weights increase monotonically from 0 to  $\frac{1}{2}Z$  as  $Za$  decreases from infinity to zero, and has an attractive inverse  $\cosh^4(x)$  component for  $|x| < a$ . For the united atom case,  $Za \downarrow 0$ ,  $v_1 + v_R = v_2 + v_R = 2v_1$  simply reproduces the molecular potential, and  $\psi_1 = \psi_2 = \psi_M$  as they should. Figure 4 displays  $v_R$  vs.  $x$  for fixed  $Z = 1$  and representative values of  $a$ . The reactivity potential is almost flat for small separations, a wide well in between the two atoms for intermediate separations, and a narrow well that is far from both atoms at large separations. Figure 5 displays the weights of the  $\delta$ -function components of  $v_R$  divided by  $Z$  vs.  $a$ .

As shown in ref.[3], the Kohn-Sham (KS) HOMO eigenvalue of each part must be identical to the chemical potential of the whole in the added presence of  $v_R$ . In our simple example, the KS potential of a part reduces to the nuclear  $\delta$ -function potential of one H atom. Adding  $v_R$  to the nuclear potential must therefore transform the HOMO energy  $E_0$ , Eq.(2.2), of the isolated atom to the more negative HOMO energy of the molecule  $E(N = 1) = -\kappa^2/2$ , which is its chemical potential (Eq.(2.8)).  $v_R$  must be attractive to do that, which it is, from Eqs.(6.9) and (6.10). In our simple example,  $v_R$  makes the delta function of the atom more negative, adds the attractive inverse  $\cosh^4$  potential between the

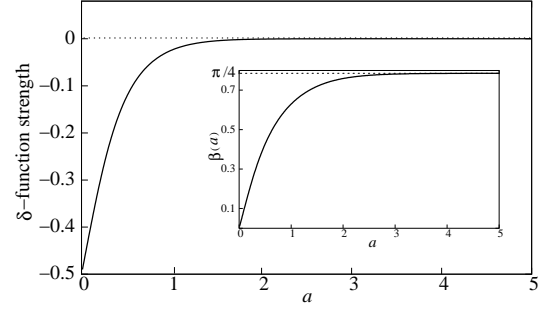


FIG. 5: Weights of the  $\delta$ -function components of  $v_R$  divided by  $Z$  as a function of  $a$  for fixed  $Z = 1$ , from the second term of Eq.(6.10). The inset shows  $\beta_a$  vs.  $a$

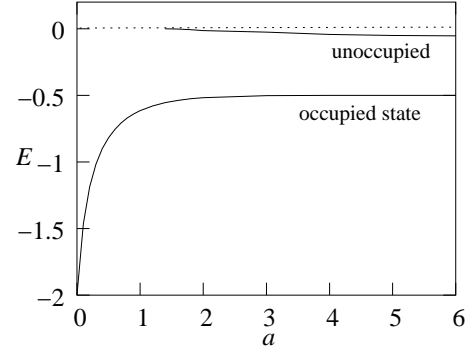


FIG. 6: Energy as a function of  $a$ , in atomic units, for the two lowest-energy solutions of Eq.(6.1).  $Z = 1$  for this plot.

atoms, and adds an attractive ghost delta function at the position of the other atom to force the wave function to decay sufficiently rapidly outside the molecule.

In the limit of infinite separation  $v_1 + v_R$  reduces to  $v_1$  and  $v_2 + v_R$  reduces to  $v_2$ , except for  $|x| < a$ , where the attractive potential

$$v_R(x) = \frac{\pi^2 E_0}{16} \frac{1}{\cosh^4 Zx} \quad , \quad |x| < a \quad , \quad (6.11)$$

persists. This potential has at least one additional bound state, but with binding energy less than  $|E_0|$ . Thus it is unoccupied, and does not affect our results. The  $a$ -dependence of this state's energy is shown for fixed  $Z$  in Fig.6. For very large separation between the atoms, it is localized at the center of the inverse  $\cosh^4(x)$  component of  $v_R$ , but it rapidly delocalizes for smaller separations. In particular, for  $Z = 1$ , it is highly delocalized when  $a < \sim 1.4$ , where it vanishes into the continuum.

## 7. SUSCEPTIBILITY AND HARDNESS

Having found the reactivity potential, we now illustrate the construction of reactivity indices. In the CRT of ref.[3], each part  $\alpha$  is represented by an ensemble of

PPLB type containing contributions with only two integer electron numbers,  $p_\alpha$  and  $p_{\alpha+1}$ . The principle of electronegativity equalization is expressed as the equality of the chemical potential of each part in the presence of the reactivity potential,  $\mu_\alpha^R$ , to the chemical potential of the molecule,  $\mu_M$ ,

$$\mu_\alpha^R = \mu_M \quad , \quad \forall \alpha \quad . \quad (7.1)$$

The  $\mu_\alpha^R$  are defined as the difference between the ground state energies of  $\alpha$  for  $p_\alpha + 1$  and  $p_\alpha$  electrons in the presence of  $v_R$ ,

$$\mu_a^R = E_\alpha^R(p_\alpha + 1) - E_\alpha^R(p_\alpha) \quad , \quad (7.2)$$

and similarly for  $\mu_M$

$$\mu_M = E_M(N_M) - E_M(N_M - 1) \quad . \quad (7.3)$$

In our simple example,  $\mu_M$  is given in Eq.(2.8). The relevant value of  $p_\alpha$  is zero, so that  $\mu_\alpha^R$  is just  $E_\alpha^R(1)$ , the lowest eigenvalue of

$$H_\alpha^R = H_\alpha + v_R \quad , \quad (7.4)$$

with  $H_\alpha$  given by Eq.(4.2) and  $v_R$  by Eq.(6.10). The explicit construction of  $v_R$  in Section 6, not possible in general, guarantees that Eq.(7.1) and therefore electronegativity equalization holds. In the general case, a modification of the Car-Parrinello scheme [14, 15] guarantees electronegativity equalization.

The susceptibility of part  $\alpha$  measures the response of the density of part  $\alpha$  to a small change in the potential  $\mathcal{V}_\alpha$  of Eq.(6.2):

$$\chi_\alpha(x, x') = -\frac{\delta n_\alpha(x)}{\delta \mathcal{V}_\alpha(x')} \quad . \quad (7.5)$$

For 2 electrons, it is simple to show that

$$\chi_\alpha(x, x') = -2\psi_\alpha(x)\mathcal{G}_\alpha(\mu_M; x, x')\psi_\alpha(x') \quad , \quad (7.6)$$

where  $\mathcal{G}_\alpha(\mu_M; x, x')$  is given by the  $E \rightarrow \mu_M$  limit of:

$$\mathcal{G}_\alpha(E; x, x') = G_\alpha(E; x, x') - \frac{\psi_\alpha(x)\psi_\alpha(x')}{E - \mu_M} \quad , \quad (7.7)$$

and  $G_\alpha$  is the Green's function for part  $\alpha$ :

$$G_\alpha(E; x, x') = \left[ E - \left( \frac{p^2}{2} + \mathcal{V}_\alpha \right) \right]^{-1} (x, x') \quad . \quad (7.8)$$

Figure 7 shows the susceptibility of the right “atom” for various interatomic separations when the perturbing potential is added at  $x_0 = 3$  (the numerical calculations were done as described in the Appendix). Electrons flow away from  $x_0$ , building up a peak at  $x_0$  (positive because of the minus sign in the definition of  $\chi_\alpha$ , Eq.(7.5)), and a negative peak at the closest maximum of the charge density, i.e. at  $a$ . With the analytic Green function of

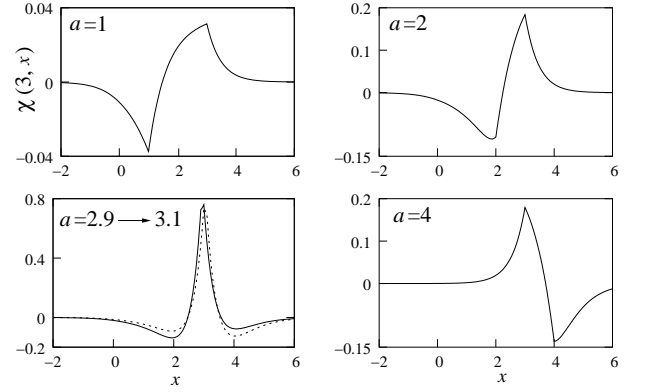


FIG. 7: Susceptibility  $\chi(x_0, x)$  of the right “atom” obtained from Eqs.(7.6)-(7.8), as indicated in the Appendix, when  $x_0$  is set to 3 a.u. Each panel corresponds to a different value of the internuclear distance,  $a$ . The lower-left panel shows  $\chi(x_0, x)$  when  $a$  is just below (solid) and just above (dotted)  $x_0$ .

an isolated “atom” [20] and Eqs.(7.6)-(7.7),  $\chi_\alpha$  can be obtained analytically in the large-separation limit:

$$\chi_\alpha(x, x') = 2e^{-Z|x|} \left\{ e^{-Z|x-x'|} - \left[ \frac{1}{2} + Z(|x| + |x'|) \right] \times e^{-Z(|x|+|x'|)} \right\} e^{-Z|x'|} \quad (7.9)$$

We now construct the susceptibility of the whole system,  $\chi_R$ , by adding together the susceptibilities of the parts,

$$\chi_R(x, x') = \sum_\alpha \chi_\alpha(x, x') \quad . \quad (7.10)$$

The inverse of  $\chi_R$  determines the hardness matrix  $\eta_{\alpha\beta}$  as shown in refs.[2] and [3]:

$$\eta_{\alpha\beta} = \int \int dx dx' f_\alpha(x) \chi_R^{-1}(x, x') f_\beta(x') \quad , \quad (7.11)$$

where the Fukui function of part  $\alpha$ ,  $f_\alpha(x)$ ,

$$f_\alpha(x) = \frac{dn_\alpha(N_\alpha, x)}{dN_\alpha} \quad , \quad (7.12)$$

is simply equal to  $\psi_\alpha^2(x)$  for 2 non-interacting electrons, since  $n_\alpha(N_\alpha, x) = N_\alpha \psi_\alpha^2(x)$  (see also ref.[16]). Thus, we have

$$\eta_{\alpha\beta} = \int \int dx dx' \psi_\alpha^2(x) \chi_R^{-1}(x, x') \psi_\beta^2(x') \quad . \quad (7.13)$$

Figure 8 shows the self-hardness  $\eta_{\alpha\alpha}$  for an isolated H-“atom”, as a function of  $Z$ . The constancy of the hardness for large  $Z$  can be understood qualitatively as follows. The inverse susceptibility has units of energy times length squared. When  $Z$  is large, it establishes a length scale inversely proportional to  $Z$ , and an energy scale

proportional to  $Z^2$ , so the  $Z$ -dependence cancels out in the inverse susceptibility. To obtain the hardness, we multiply  $\chi_R^{-1}$  on the left and right by the Fukui function, which has the dimension of inverse length. Integrating over position on the left and right then cancels out the  $Z$ -dependence arising from the Fukui functions, and the result is a  $Z$ -independent hardness.

## 8. CONCLUSIONS

Despite the extreme simplicity of the 1D-H2 model analyzed here – two non-interacting electrons moving in 1D under the influence of two equivalent attractive delta-function potentials – that model allows us to illustrate the essential features of our partition theory and of key indices of our chemical reactivity via straightforward analysis and easy computations.

We have shown that the electron density of the molecule can be decomposed exactly into a sum of atomic densities, a rigorous solution of the “atoms-in-molecules” problem [17].

Electronegativity equalization [18] is built into the partition by the symmetry of the problem, so this homonuclear model does not illustrate that principle as well as a heteronuclear model would. Nevertheless, the current example does illustrate a key feature of the new CRT, the chemical context dependence of the reactivity indices, in this case the electronegativity of a part, introduced through the presence of  $v_R$  in the Schrödinger equation for  $\psi_\alpha$ , cf. Eq.(7.4). It also demonstrates that the reactivity potential remains finite as two atoms separate, but has no effect on the partitioning after separation.

Another serious shortcoming of the earlier formulations of DFT-based CRT is the vanishing of the hardness. We have shown explicitly here that the self-hardness, as defined in [3], of an isolated “atom” is positive. Interestingly, the hardness saturates as the ionization energy of the “atom” increases, raising the very interesting question of whether such a saturation of hardness with ionization energy exists in real systems. For this model, a strong positive correlation between hardness and ionization energy exists only over the limited range of  $Z$  between 0.4 and 0.7.

KB is supported by NSF CHE-0355405.

## APPENDIX: Numerical calculation of the susceptibility

We first obtained  $G_\alpha(E; x, x')$  according to the well-known prescription [19]:

$$G_\alpha(E; x, x') = 2 \frac{\psi_{\alpha,L}(E, x_{<})\psi_{\alpha,R}(E, x_{>})}{W[\psi_{\alpha,L}, \psi_{\alpha,R}]}, \quad (\text{A.1})$$

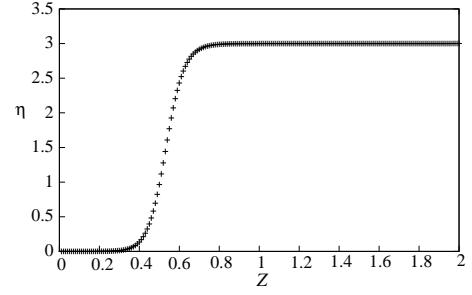


FIG. 8: Self-hardness vs.  $Z$  in the separated-atom limit (atomic units).

where  $x_{<} = \inf(x, x')$ ,  $x_{>} = \sup(x, x')$

$$W[\psi_{\alpha,L}, \psi_{\alpha,R}] = \psi_{\alpha,L}(E, x)\psi'_{\alpha,R}(E, x) - \psi'_{\alpha,L}(E, x)\psi_{\alpha,R}(E, x), \quad (\text{A.2})$$

and the orbitals  $\psi_{\alpha,L}$  and  $\psi_{\alpha,R}$  are solutions of

$$\left[ \frac{p^2}{2} + \mathcal{V}_\alpha(x) \right] \psi_{\alpha,L,R}(E, x) = E\psi_{\alpha,L,R}(E, x) \quad (\text{A.3})$$

satisfying left and right-boundary conditions, respectively:

$$|\psi_{\alpha,L}(E, x)| \downarrow 0 \quad , \quad x \downarrow -\infty \quad (\text{A.4})$$

$$|\psi_{\alpha,R}(E, x)| \downarrow 0 \quad , \quad x \uparrow \infty \quad (\text{A.5})$$

The potential  $\mathcal{V}_\alpha(x)$  of Eq.(A.3) is given by Eq.(6.2), with the reactivity potential  $v_R(x)$  of Eq.(6.10). The computations of  $\psi_{\alpha,L,R}(E, x)$  were carried out at  $E = \mu_M \pm \Delta E$  with  $\Delta E$  chosen for numerical convenience, i.e. large enough so that  $\sup_{x,x'} |G_\alpha(\mu_M \pm \Delta E)|$  does not become so large as to be inconvenient on the one hand, and small enough so that  $\frac{1}{2} [G_\alpha(\mu_M + \Delta E) + G_\alpha(\mu_M - \Delta E)]$  does not differ significantly from its limit at  $\Delta E \downarrow 0$ . We then calculated  $\mathcal{G}_\alpha$  of Eq.(7.7) as:

$$\mathcal{G}_\alpha(\mu_M; x, x') = \frac{1}{2} [G_\alpha(\mu_M + \Delta E; x, x') + G_\alpha(\mu_M - \Delta E; x, x')] \quad (\text{A.6})$$

- 
- [1] M.H. Cohen and A. Wasserman, Israel J. Chem. **43**, 219 (2003).
- [2] M.H. Cohen and A. Wasserman, J. Stat. Phys. **125**, 1125 (2006).
- [3] M.H. Cohen and A. Wasserman, J. Phys. Chem. A **111**, 2229 (2007).
- [4] P. Hohenberg and W. Kohn, Phys. Rev. **136B**, 864 (1964).
- [5] W. Kohn and L.J. Sham, Phys. Rev. **140**, A1133 (1965).
- [6] M. Levy, Proc. Nat. Acad. Sci. USA **76**, 6062 (1979).
- [7] E.H. Lieb, in *Physics as Natural Philosophy*, eds. A. Shimony, and H. Feshbach, MIT Press, Cambridge, p.111 (1982).
- [8] J.P. Perdew, R.G. Parr, M. Levy, and J.R. Balduz, Jr., Phys. Rev. Lett. **49**, 1691 (1982).
- [9] J.P. Perdew, in *Density Functional Methods in Physics*, ed. R.M. Dreizler and J. da Providencia, Plenum, New York, p.265 (1985).
- [10] R. Parr and W. Yang, *Density Functional Theory of Atoms and Molecules*, Oxford University Press, New York (1989).
- [11] P. Geerlings, F. De Proft, and W. Langenaeker, *Chem. Rev.* **103**, 1793 (2003).
- [12] R.G. Parr, R.A. Donnelly, M. Levy, and W.E. Palke, J. Chem. Phys. **68**, 3801 (1978).
- [13] R.G. Parr and R.G. Pearson, J. Am. Chem. Soc. **105**, 7512 (1983).
- [14] R. Car and M. Parrinello, Phys. Rev. Lett. **55**, 2471 (1985).
- [15] M.H. Cohen and R. Car, unpublished.
- [16] P. Fuentealba, E. Chamorro, and C. Cárdenas, Int. J. Quant. Chem. **107**, 37 (2007).
- [17] F.L. Hirshfeld, Theor. Chim. Acta **44**, 129 (1977); R. F. W. Bader, *Atoms in Molecules - A Quantum Theory*, Oxford University Press, Oxford, 1990.; R.F. Nalewajski and R.G. Parr, Proc. Natl. Acad. Sci. USA **97**, 8879 (2000).
- [18] R.T. Sanderson, Science **114**, 670 (1951).
- [19] G. Arfken, *Mathematical Methods for Physicists*, Academic Press, New York (1970).
- [20] A. Szabo and N.S. Ostlund, *Modern Quantum Chemistry: Introduction to Advanced Electronic Structure Theory*, McGraw-Hill, New York (1989).